Available online at www.sciencedirect.com
SCIENCE DIRECT®
Electrochemistry Communications 8 (2006) 1197–1203
electrochemistry communications
www.elsevier.com/locate/elecom

Electrodeposition of silver–DNA hybrid nanoparticles for electrochemical sensing of hydrogen peroxide and glucose

Shuo Wu, Hongtao Zhao, Huangxian Ju *, Chuanguo Shi, Jianwei Zhao

Key Laboratory of Analytical Chemistry for Life Science, (Ministry of Education of China) School of Chemistry and Chemical Engineering, Nanjing University, Nanjing 210093, PR China

Received 25 April 2006; received in revised form 21 May 2006; accepted 22 May 2006
Available online 30 June 2006

Abstract

Silver–DNA hybrid nanoparticles with controlled dimension were electrodeposited on a glassy carbon electrode by the reduction of silver in the aid of DNA. The hybrid nanoparticles showed a narrow size distribution and a favorable catalytic ability to reduction of hydrogen peroxide and dissolved oxygen, which were related to the DNA concentration in deposition solution and the deposition time. The presence of DNA avoided the further aggregation of silver nanoparticles and improved the catalytic ability of the nanoparticles. The modified electrode obtained showed a linear response to hydrogen peroxide concentration ranging from 2.0 μM to 2.5 mM with a limit of detection of 0.6 μM and a sensitivity of 773 μA mM^{-1} cm^{-2}. Based on the dissolved oxygen consumption during the oxidation process of glucose catalyzed by the immobilized glucose oxidase, a glucose biosensor with a limit of detection of 9.0 μM and a linear range from 50 μM to 1.2 mM was fabricated. The biosensor excluded the interference from ascorbic acid, acetaminophen, and uric acid that always coexist with glucose in samples.

Keywords: Nanoparticles; Electrodeposition; Silver–DNA hybrid nanoparticles; Amperometric biosensors; Hydrogen peroxide

1. Introduction

Nanoparticles, especially the noble-metal nanoparticles, have attracted considerable attention in constructing electrochemical or optical sensors due to their small sizes and correspondingly unique electronic [1], optical [2], and catalytic properties [3]. Recently, electrochemical sensors based on nanomaterials such as gold [4], silver [1], platinum [5], copper [6], and metal oxide [7] have been widely used in environment, food and clinical fields owing to the inherent properties such as inexpensive, portable, high sensitivity, and high selectivity [8]. As a typical nanoparticle used in biosensing, the silver nanoparticle with controllable dimension and size distribution has aroused much interest, due to its excellent surface-enhanced Raman scattering (SERS) [9] and catalytic [10] activity.

Several methods including chemical reduction of silver cation in presence of stabilizers [11–13], layer-by-layer adsorption [14], template induction [15–19], photo-irradiation [20], seed-mediated synthesis [19], electroless preparation [20], and electrochemical deposition [10,21–24] have been developed for the preparation of silver nanoparticles. The deposition of silver nanoparticle on indium tin oxide and gold electrodes has been achieved by chemical reaction with a seed-mediated process [25] and layer-by-layer alternative adsorption of positively charged polyelectrolyte-silver ion complex and negatively charged polyelectrolyte coupled with heating or exposure to NaBH4 [14], respectively. The as-prepared surfaces possess good electrocatalytic properties. In view of the importance of direct preparation of silver nanoparticle-attached functional surface for its practical application, this work presented a new simple and direct method for preparation of silver nanoparticle-attached functional surface by electrodeposition of silver cations–DNA complex on a glassy carbon

* Corresponding author. Tel./fax: +86 25 83593593.
E-mail address: hxju@nju.edu.cn (H. Ju).

1388-2481/$ - see front matter © 2006 Elsevier B.V. All rights reserved.
doi:10.1016/j.elecom.2006.05.013

electrode. The presence of DNA template prevented the aggregation of silver nanoparticles.

The electrocatalytic properties of the silver nanoparticles depend on their dimension and amount deposited on electrode surface. By applying a reduction potential followed by anodic stripping a relatively wider size distribution of silver particles has been obtained [10,25]. The sizes of the silver particles are 0.1–1.0 μm, 0.25–0.5 μm, and 100 nm after stripping for 1, 2, and 5 min, respectively [10]. Although the nano-sized silver particles ranging from 5 to 50 nm have been obtained after a stripping period of 10 min, the particle density is very low [25], which is unfavorable for the electrocatalysis and sensing application of silver nanoparticles [10]. This work prepared *in situ* silver–DNA hybrid nanoparticles with controllable dimension on electrode surface by adding DNA as a template in the deposition solution. Although DNA has been used as a natural template for growing nanowires and nanoparticles by chemical reduction [17–19,26] or electrochemical reduction assisted with ultrasonic [27], it was used for the first time for *in situ* electrochemical preparation of the silver–DNA hybrid nanoparticles for sensing purpose. The obtained nanoparticles showed excellent electrocatalytic activity to reduction of both hydrogen peroxide and oxygen at relatively low overpotentials. The hydrogen peroxide sensor possessed both low detection limit and wide linear range, showing good analytical performance and practicability. By immobilizing glucose oxidase on the nanoparticles modified electrode with organic modified sol–gel (ormosil) to prepare a glucose biosensor, the practicability of the obtained hybrid nanoparticles was verified.

2. Experimental

2.1. Materials

Salmon sperm DNA, glucose oxidase (GOx, EC 1.1.3.4, Type X.S from *Aspergillus niger*), β-D(+)-glucose, polyethylene and glycol (PEG) were all purchased from Sigma–Aldrich (USA). 2-(3,4-epoxycyclohexyl)-ethyltrimethoxysilane (Epoxy) and (3-aminopropyl) triethoxysilane (APTES) were obtained from Fluka Chemie, GmbH. Other reagents were of analytical reagent grade. Phosphate buffer saline (PBS) was prepared by mixing the stock solutions of NaH_2PO_4 and Na_2HPO_4. Doubly distilled water was used in all experiments.

2.2. Electrodeposition of silver–DNA modified electrode

The glassy carbon electrodes were firstly polished to a mirror finish with 0.3 and 0.05 μm alumina slurry (Beuhler) followed by thoroughly rinsing with deionized water. The silver–DNA hybrid nanoparticles were electrodeposited on the electrodes in 0.1 M KNO_3 solution containing 3.0 mM $AgNO_3$ + 0.5 mg mL^{-1} DNA at −0.1 V (vs. Ag/AgCl) for different times to obtain nanoparticles modified electrodes. As control, two types of modified electrodes were obtained by electrodeposition in 0.1 M KNO_3 solution containing 3.0 mM $AgNO_3$ for 10 s and 350 s and 1.0 mM $AgNO_3$ for 30 s.

2.3. Preparation of glucose biosensors

25.0 μL solution of PEG (4.0% w/v), 17.0 μL APTES, and 9.0 μL Epoxy were added sequentially to 125.0 μL water and mixed thoroughly on stirrer. After 2 min 2.0 μL of 0.1 M HCl was added to the mixture and stirred again for 30 s. Then 10.0 μL GOx (4698.0 IU mL^{-1} in pH 7.0 PBS) was added to the mixture on stirrer. Immediately, 3.0 μL of the obtained mixture was cast on the silver–DNA hybrid nanoparticles modified electrode that was prepared by electrodeposition for 180 s. The surface was allowed for the condensation at room temperature for 3 h to form a Ag–DNA/ormosil/GOx composite film-based glucose biosensor.

2.4. Electrochemical measurements and apparatus

All electrochemical measurements were performed on a CHI 660B electrochemical workstation (CH Instruments Inc., USA) with a conventional three-electrode system comprised of a platinum wire as auxiliary, Ag/AgCl and SCE as reference for electrodeposition and electrochemical measurements, respectively, and glassy carbon electrode (GCE, 3 mm in diameter, CH Instruments Inc., USA) as working electrodes. Hydrogen peroxide detection were performed in PBS bubbled with nitrogen for more than 30 min to exclude the oxygen interference. The electrochemical response of the glucose biosensor was detected with in PBS in air.

X-ray photoelectron spectra (XPS) were recorded on an ESCALAB MKII X-ray photoelectron spectrometer, using nanomonochromatized Mg Kα X-ray as the excitation source and C1s (284.6 eV) as the reference line. Atomic force microscopic (AFM) plots were obtained in ambient conditions using a Molecular Imaging Pico SPM (USA) in tapping mode with a 10 μm scanner.

3. Results and discussion

3.1. Electrodeposition of silver–DNA hybrid nanoparticles

Fig. 1A showed the effect of DNA on the redox behaviors of Ag^+ at a glassy carbon electrode. The cyclic voltammogram of $AgNO_3$ showed a cathodic peak at −0.105 V (vs. Ag/AgCl), which resulted from the reduction of Ag^+ diffusing from solution to the electrode surface. The anodic process showed a sharp peak at +0.096 V, which was attributed to the stripping of the electrodeposited silver. After the addition of DNA to the Ag^+ solution, the redox peak currents decreased and the peak potentials shifted in negative direction due to the formation of the Ag^+–DNA complexes [17] and the electrostatic interaction between negatively charged phosphate groups of DNA strand and

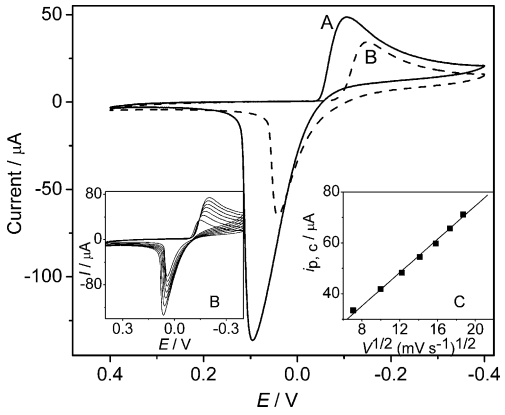

Fig. 1. Cyclic voltammograms of 3.0 mM $AgNO_3$ + 0.1 M KNO_3 solution containing 0 (A) and 0.5 (B) mg mL^{-1} DNA at 50 mV s^{-1}. Insets: cyclic voltammograms of B solution at 50, 100, 150, 200, 250, and 300 mV s^{-1} (from low to high) and plot of reduction peak current vs. the square root of scan rate.

Ag^+. These processes lowed the diffusion coefficient of electroactive species and made the reduction of Ag^+ more difficult. In the studied range of scan rate, the cathodic peak current was proportional to the square root of scan rate and the cathodic peak potential shifted slightly in negative direction (Fig. 1B and C), indicating a quasi-reversible electrode process. The reduction of the Ag^+–DNA complex resulted in the formation of silver–DNA hybrid nanoparticles.

As shown in Fig. 2A, after electrodeposition of 3.0 mM $AgNO_3$ at −0.1 V (vs. Ag/AgCl) for 10 s a film of silver particles with the thickness less than 100 nm was formed. Both the distribution and size of these particles were uneven. The diameters of silver blocks were from 100 to 500 nm, indicating that the silver atoms produced from the reduction of Ag^+ cations grew on the deposited silver nucleus to form large blocks. Upon addition of 0.5 mg mL^{-1} DNA to the solution the electrodeposition of 10 s produced a uniformly distributed film of silver–DNA hybrid nanoparticles (Fig. 2B). The diameter of the formed hybrid nanoparticles was less than 50 nm. The film thickness was 300–500 nm, which was much larger than both the diameter of the formed hybrid nanoparticles and the film thickness formed in the absence of DNA. The larger thickness of the film resulted from the presence of folded DNA strand in the hybrid nanoparticles.

With the increasing electrodeposition time the thickness of the formed film increased and the size of the formed silver–DNA hybrid nanoparticles showed only small change (Fig. 2C). The presence of DNA avoided the further aggregation of the nanoparticles, though more silver was deposited on the electrode surface. Attractively, the dimension of the as-synthesized silver nanoparticles was less and their distribution was more uniform than those electrodeposited in $AgNO_3$ solution with the presence of KCN by a double pulse method [21], in $AgNO_3$ solution by cathodic reduction followed with anodic stripping technique [10,25], and in room temperature ionic liquids containing $AgBF_4$ at 0.36 V (vs. Ag/AgCl) for 60 min [22].

Fig. 3 showed the XPS of the nano-sized nanoparticles, which were thoroughly washed with deionized water to remove the physically adsorbed DNA. Typical peaks at 147.30, 298.45, 413.65, 544.60, and 381.95 eV were attrib-

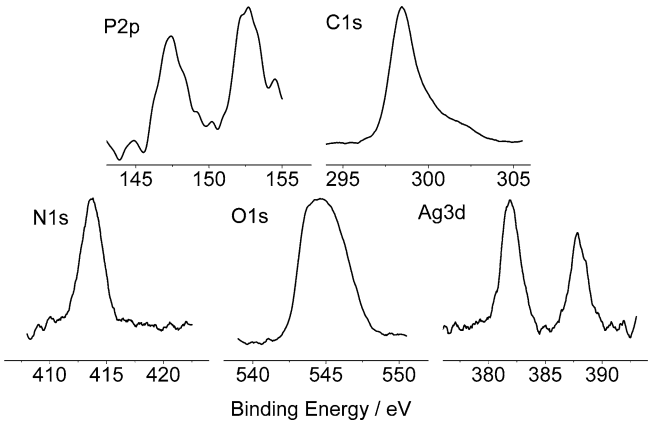

Fig. 3. X-ray photoelectron spectra of silver–DNA hybrid nanoparticles obtained in 0.1 M KNO_3 solution containing 0.5 mg mL^{-1} DNA + 3.0 mM $AgNO_3$ at −0.1 V for 350 s.

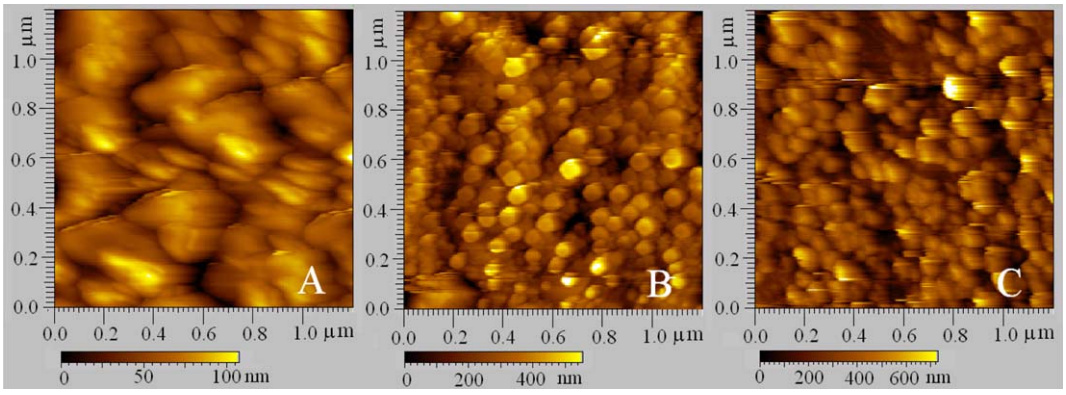

Fig. 2. AFM surface plots of nanoparticles obtained at −0.1 V in 0.1 M KNO_3 solution containing 3.0 mM $AgNO_3$ for 10 s (A) and 3.0 mM $AgNO_3$ + 0.5 mg mL^{-1} DNA for 10 (B) and 30 s (C).

uted to P2p, C1s, N1s, O1s, and Ag3d, respectively, which indicated that DNA molecules were coexisted with silver in the formed silver–DNA hybrid nanoparticles.

Interestingly, in the absence of DNA no nanostructure could be observed on the electrode surface even when a low $AgNO_3$ concentration was used in the electrodepositing process. The AFM surface plot of a film obtained in 1.0 mM $AgNO_3$ at −0.1 V (vs. Ag/AgCl) for 30 s showed several isolated blocks with dimension ranging from 200 to 700 nm (Fig. 4A). Comparatively, a film with homogenously distributed nanoparticles was obtained at the same applied potential with the same period when DNA was added to the $AgNO_3$ solution, even if a higher $AgNO_3$ concentration was used (Fig. 4B). The results further verified that DNA was crucial for the final formation of the homogenously distributed nano-sized nanoparticles.

3.2. Response to hydrogen peroxide

Fig. 5 (left) shows the cyclic voltammograms of 0.6 mM H_2O_2 at bare (A), silver particles (B), and silver–DNA hybrid nanoparticles (C) modified electrodes. The Ag/GCE and Ag–DNA/GCE were prepared by electrodeposition in 0.1 M KNO_3 solution containing 3.0 mM $AgNO_3$ without and with 0.5 mg mL^{-1} DNA at −0.1 V (vs. Ag/AgCl) for 350 s, respectively. The bare GCE did not show any observable response in the studied potential range. At the Ag/GCE an obvious peak resulted from the reduction of H_2O_2 was observed at −540 mV, indicating the promotion of silver particles to H_2O_2 reduction. This peak occurred at −444 mV at the Ag–DNA/GCE. Obviously, the close packed silver–DNA hybrid nanoparticles showed lower overpotential for H_2O_2 reduction, thus possessed stronger catalytic ability to H_2O_2 reduction than the Ag/GCE, which resulted from two factors. One was the smaller size and larger total surface area of the nanoparticles, which produced more active sites on electrode surface and made them easier to contact with H_2O_2 substrate. In addition, the size influence of nanoparticles on the catalytic ability could be explained according to the microelectrode theory. The modified electrode composed of many nanoparticles without aggregation could be treated as an integration of many small silver nanoelectrodes. Compton [10] compared the amperometric responses of a

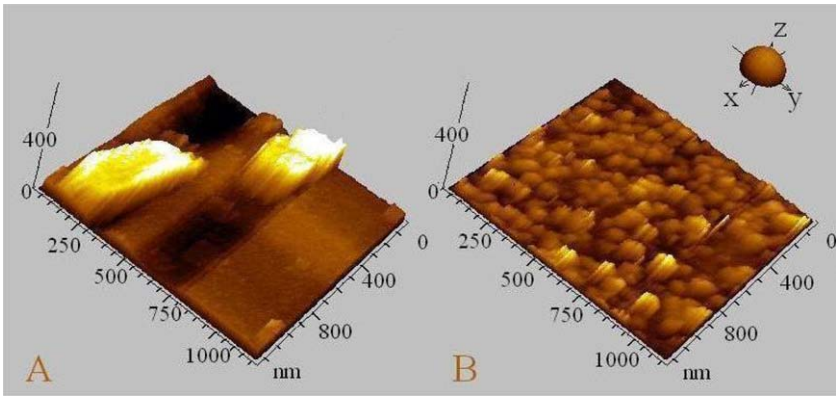

Fig. 4. AFM surface plots of nanoparticles obtained in 0.1 M KNO_3 solution containing 1.0 mM $AgNO_3$ (A) and 3.0 mM $AgNO_3$ + 0.5 mg mL^{-1} DNA (B) at −0.1 V for 30 s.

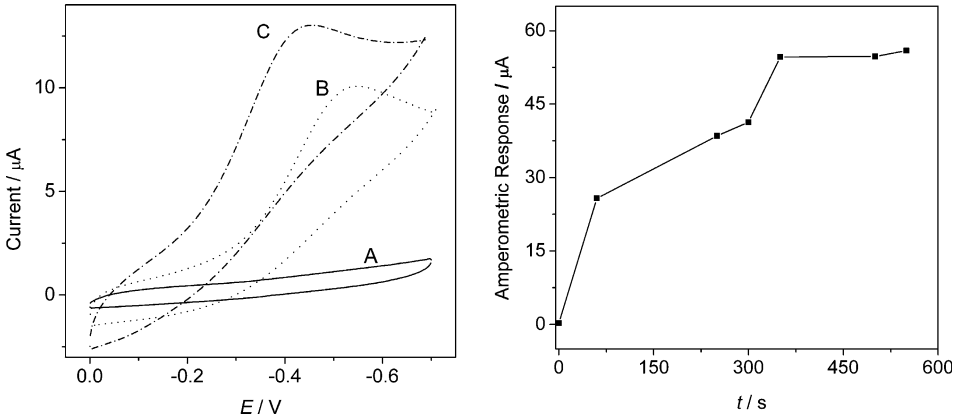

Fig. 5. Cyclic voltammograms of GCE (A), Ag/GCE (B) and Ag–DNA/GCE (C) in 0.2 M pH 7.0 PBS containing 600 μM H_2O_2 at 50 mV s^{-1} (left) and effect of deposition time on amperometric response of the Ag–DNA/GCE to 1.0 mM H_2O_2 in 0.2 M pH 7.0 PBS (right).

macroelectrode with a surface area of 1 cm^2 with an array of electrodes with the same geometric area comprising separate electrodes. The amperometric response of the electrode array with radius of 1 μM, 100 nm, and 10 nm were 20, 200, and 2000 times larger than that at the macroelectrode, respectively. Therefore, the electrocatalytic ability increased when the nanosize decreased if the electrode surface was fully covered with nanoparticles. Another factor was the presence of DNA strands in the hybrid nanoparticles, which led to a catalytic activity similar to that of carbon nanotube, at which the hydrogen peroxide could be reduced at about −400 mV [28]. The strong catalytic activity of the silver–DNA hybrid nanoparticles led to greater reduction peak current of H_2O_2 than at the Ag/GCE, resulting in higher sensitivity for detection of H_2O_2 at a relatively low overpotential.

With the increasing deposition time the amperometric response to H_2O_2 at −450 mV increased and trended to a maximum value after a deposition time of 350 s (Fig. 5 right), which was chosen for preparation of the Ag–DNA/GCE used for H_2O_2 sensing.

The applied potential for amperometric detection of H_2O_2 was selected according to its amperometric response to 100 μM H_2O_2. Hydrogen peroxide began to be reduced on the Ag–DNA/GCE at an applied potential of −200 mV. With the negative shift of the applied potential the response increased and reached a plateau at −450 mV, which was used for the amperometric detection of H_2O_2.

The effect of DNA concentration in the deposition solution containing 3.0 mM $AgNO_3$ on the amperometric response of H_2O_2 was examined in the concentration range of 0–2.0 mg mL^{-1}. The maximum response occurred at the DNA concentration of 0.5 mg mL^{-1}, which was 2.5 times larger than that in the absence of DNA. After DNA concentration was larger than 0.5 mg mL^{-1} the amperometric decreased. This might be due to the fact that the high DNA content in the hybrid nanoparticles decreased the packing density and electric conductivity of the nanoparticles. Thus 0.5 mg mL^{-1} DNA was used for electrodeposition of 3.0 mM $AgNO_3$ to prepare the H_2O_2 sensor.

3.3. Sensing application to hydrogen peroxide detection

Fig. 6 shows the amperometric response of the Ag–DNA/GCE to the successive addition of H_2O_2 of different concentrations at −450 mV. The upper current–time curve followed the lower curve due to the overflow of the first part. Upon each addition of H_2O_2 the Ag–DNA/GCE reached the maximum response within 4 s, indicating a rapid amperometric response. The response was proportional to the H_2O_2 concentration in a range from 2.0 μM to 2.5 mM with a slope of 54.6 μA mM and a correlation coefficient of 0.9997 ($n = 31$), as shown in Fig. 6 inset A. The sensitivity was 773 μA mM^{-1} cm^{-2}, which was higher than those of 0.2 A M^{-1} cm^{-2} at nanostructured prussian blue modified electrode [29], and 43.6 μA mM^{-1} cm^{-2} at platinum nanoparticle embedded carbon film electrode

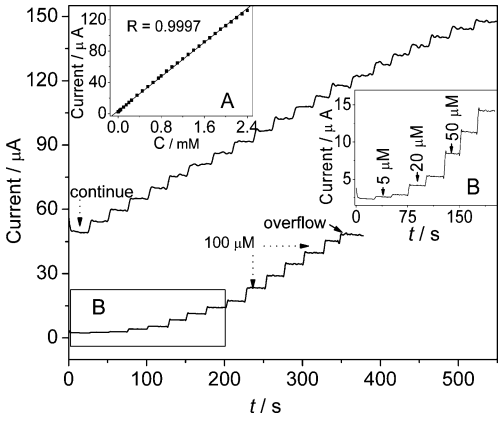

Fig. 6. Current–time curve of the silver–DNA hybrid nanoparticle modified electrode for successive addition of H_2O_2 with marked concentrations to 0.2 M pH 7.0 PBS at −0.45 V. Inset A: calibration curve for H_2O_2. Inset B: amplification of curve B.

[5]. The limit of detection was estimated from the slope to be 0.6 μM at a signal-to-noise ratio of 3, which was lower than that of 2 μM at a silver nanoparticle modified glassy carbon electrode [10]. In comparison with the upper limit of 64 μM at an enzyme modified biosensors [30], the linear range for detection of H_2O_2 extended three orders of magnitude, showing better practicability. The intra- or inter-assay coefficients of variation for five successive determinations of 0.8 mM H_2O_2 and five detections of 0.1 mM H_2O_2 at five electrodes prepared independently were 1.7% and 6.1%, respectively, indicating acceptable fabrication reproducibility.

3.4. Response to oxygen and sensing application to glucose

Fig. 7 shows the cyclic voltammograms of the bare GCE (A) and Ag–DNA/GCE (B) in air saturated 0.1 M pH 7.0 PBS. At Ag–DNA/GCE dissolved oxygen began to reduce at about −100 mV and the cyclic voltammograms showed an obvious reduction peak centered at about −330 mV, while the oxygen began to reduce after −400 mV and no

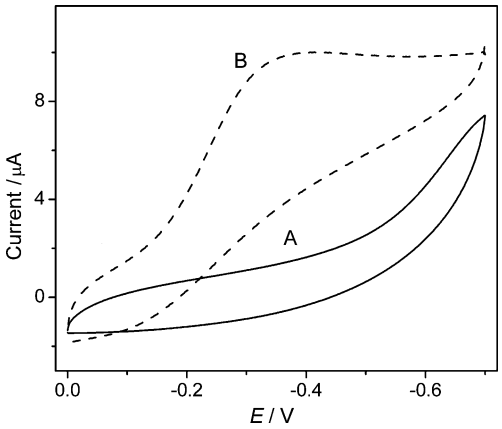

Fig. 7. Cyclic voltammograms of GCE (A), and Ag–DNA/GCE (B) modified electrode in 0.1 M pH 7.0 air saturated PBS at 50 mV s^{-1}.

reductive peak was observed in the scan range at the bare GCE. The oxygen electroreductive potential was comparable with those obtained at the carbon nanotubes modified electrode [31].

Based on the high catalytic activity and biocompatibility of the silver–DNA hybrid nanoparticles, a glucose biosensor was fabricated with the introduction of glucose oxidase by ormosil to the surface of the Ag–DNA/GCE. The oxidation process of glucose by dissolved oxygen during enzymatically reaction could produce hydrogen peroxide, leading to the increase of hydrogen peroxide concentration and the decrease of dissolved oxygen concentration on the silver–DNA hybrid nanoparticle modified electrode. These changes produced two opposite changes of the electrocatalyzed amperometric responses to the reduction of dissolved oxygen and hydrogen peroxide. They could be used for detection of glucose. However, the reduction of hydrogen peroxide needed more negative potential (−450 mV) than that of oxygen (−300 mV). Therefore, this work used the consumption of dissolved oxygen to detect glucose at a relatively favorable potential for excluding the interference of other coexisted species.

Fig. 8 shows the amperometric response of the biosensor to the successive addition of glucose to the air saturated stirring 0.1 M pH 7.4 PBS at −300 mV, which was chosen according to the best signal-to-noise factor. A subsequent addition of glucose resulted in a decrease in the amperometric response of dissolved oxygen. The time required to reach the 95% steady state response was within 5 s. The linear calibration range for glucose was 0.05–1.2 mM ($r = 0.999$, $n = 12$) with a limit of detection of 9.0 μM (Fig. 8 inset). The sensitivity was 38.3 μA mM^{-1} cm^{-2}, which is higher than that of 14.2 μA mM^{-1} cm^{-2} on an oxygen sensitive carbon nanotubes modified electrode [32].

The biosensor also showed good selectivity for glucose. In 0.05 mM glucose solution the responses caused by 0.2 mM acetaminophen (AP), uric acid (UA), and 0.5 mM ascorbic acid (AA) were negligible.

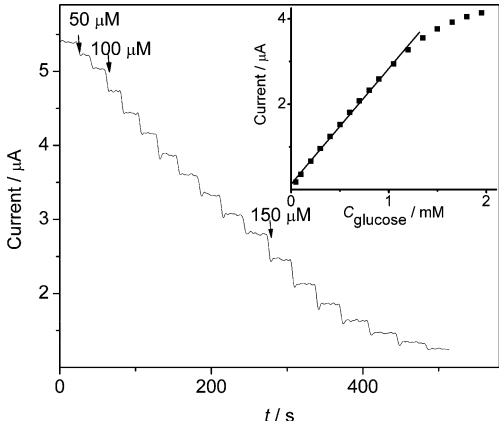

Fig. 8. Current–time curve of the Ag–DNA/ormosil/GOx modified electrode for successive addition of glucose with marked concentrations to 0.1 M pH 7.4 PBS at −0.3 V. Inset: calibration curve for glucose.

4. Conclusions

Silver–DNA hybrid nanoparticles are prepared on an electrode surface by electro-reductive deposition of Ag^+–DNA complex. The strong association of Ag^+ with DNA makes the reduction of silver cation more difficult, thus the reduction peak potential shifts in negative direction. The formed hybrid nanoparticles show a narrow size distribution with a dimension of around 50 nm in diameter. The presence of DNA is a key factor for the formation of homogenously distributed nano-sized nanoparticles and avoids the further aggregation of the nanoparticles upon the increasing electrodeposition time. Long electrodeposition time results in an increase in the film thickness. Such silver–DNA hybrid nanoparticles show good catalytic ability to the reduction of hydrogen peroxide and oxygen, thus produce good sensitivity for rapid detection of hydrogen peroxide in the absence of oxygen with a wide linear range and acceptable reproducibility. Based on the good catalytic ability and the biocompatibility of the silver–DNA hybrid nanoparticle, a glucose biosensor with high sensitivity was fabricated in the help of ormosil for the immobilization of GOx. Comparing with other electrochemical deposition methods, this proposed method is effective for preparation of well-dispersed nanoparticles modified functional surfaces, which could be applied in the synthesis of other metal nanoparticles.

Acknowledgements

We gratefully acknowledge to the National Science Funds for Distinguished Young Scholars (20325518) and Creative Research Groups (20521503), the Key Program (20535010) from the National Natural Science Foundation of China and the Creative Program for Postgraduates in University from Education Office of Jiangsu for financial support of this research.

References

[1] X.L. Rena, X.W. Menga, D. Chena, F. Tanga, J. Jiao, Biosens. Bioelectron. 21 (2005) 433.
[2] J.W. Zheng, X.W. Li, R. Gu, T.H. Lu, J. Phys. Chem. B 106 (2002) 1019.
[3] W. Yantasee, L.A. Deibler, G.E. Fryxell, C. Timchalk, Y.H. Lin, Electrochem. Commun. 7 (2005) 1170.
[4] J. Weng, J.M. Xue, J. Wang, J.S. Ye, H.F. Cui, F.S. Sheu, Q.Q. Zhang, Adv. Funct. Mater. 15 (2005) 639.
[5] T.Y. You, O. Niwa, M. Tomita, S. Hirono, Anal. Chem. 75 (2003) 2080.
[6] H.Y. Wang, Y.G. Huang, Z.A. Tan, X.Y. Hu, Anal. Chim. Acta 526 (2004) 13.
[7] G.D. Liu, Y.H. Lin, Anal. Chem. 77 (2005) 5894.
[8] J. Wang, Analyst 130 (2005) 421.
[9] K. Kim, H.S. Lee, J. Phys. Chem. B 109 (2005) 18929.
[10] C.M. Welch, C.E. Banks, A.O. Simm, R.G. Compton, Anal. Bioanal. Chem. 382 (2005) 12.
[11] K.C. Beverly, J.F. Sampaio, J.R. Heath, J. Phys. Chem. B 106 (2002) 2131.
[12] J. Zhang, C.D. Geddes, J.R. Lakowicz, Anal. Biochem. 332 (2004) 253.

[13] Y. Lu, G.L. Liu, L.P. Lee, Nano Lett. 5 (2005) 5.
[14] J.H. Dai, M.L. Bruening, Nano Lett. 2 (2002) 497.
[15] Z.P. Zhang, M.Y. Han, J. Mater. Chem. 13 (2003) 641.
[16] M. Andersson, J.S. Pedersen, A.E.C. Palmqvist, Langmuir 21 (2005) 11387.
[17] J.T. Petty, J. Zheng, N.V. Hud, R.M. Dickson, J. Am. Chem. Soc. 126 (2004) 5207.
[18] A. Kumar, V. Ramakrishnan, R. Gonnade, K.N. Ganesh, M. Sastry, Nanotechnology 13 (2002) 597.
[19] S. Behrens, J. Wu, W. Habicht, E. Unger, Chem. Mater. 16 (2004) 3085.
[20] S. Eustis, G. Krylova, A. Eremenko, N. Smirnova, A.W. Schilla, M. El-Sayed, Photochem. Photobiol. Sci. 4 (2005) 154.
[21] G. Sandmann, H. Dietz, W. Plieth, J. Electroanal. Chem. 491 (2000) 78.
[22] P. He, H.T. Liu, Z.Y. Li, Y. Liu, X.D. Xu, J.H. Li, Langmuir 20 (2004) 10260.
[23] Y.C. Liu, L.H. Lin, Electrochem. Commun. 6 (2004) 1163.
[24] M. Mazur, Electrochem. Commun. 6 (2004) 400.
[25] K.H. Ng, H. Liu, R.M. Penner, Langmuir 16 (2000) 4016.
[26] E. Braun, Y. Eichen, U. Sivan, G. Ben-Yoseph, Nature 391 (1998) 775.
[27] J.J. Zhu, X.H. Liao, H.Y. Chen, Mater. Res. Bull. 36 (2001) 1687.
[28] J. Wang, M. Musameh, Y.H. Lin, J. Am. Chem. Soc. 125 (2003) 2408.
[29] E.A. Puganova, A.A. Karyakin, Sensor. Actuat. B-Chem. 109 (2005) 167.
[30] Y.F. Yang, S.L. Mu, Biosens. Bioelectron. 21 (2005) 74.
[31] M.N. Zhang, Y.M. Yan, K.P. Gong, L.Q. Mao, Z.X. Guo, Y. Chen, Langmuir 20 (2004) 8781.
[32] Y.Q. Dai, K.K. Shiu, Electroanalysis 16 (2004) 1697.